SORPTION OF Cu²⁺ FROM AQUEOUS SOLUTIONS BY SLOVAK BENTONITES

#ANNA BRTÁŇOVÁ, ZUZANA MELICHOVÁ*, PETER KOMADEL

Institute of Inorganic Chemistry, Slovak Academy of Science,
Dúbravská cesta 9, Bratislava 845 36, Slovak Republic
*Department of Chemistry, Faculty of Natural Sciences, Matej Bel University,
Tajovského 40, Banská Bystrica 974 01, Slovak Republic

#E-mail: anna.brtanova@savba.sk

Bentonites are used as barriers in landfills, or in areas of old mining activities to prevent contamination of environment by leachates containing heavy metals. Batch experiments were performed under static conditions to study sorption of Cu²⁺ from aqueous solutions via adsorption on industrial products made from Slovak bentonites Lieskovec and Jelšový Potok. The samples were characterized by X-ray powder diffraction, infrared spectroscopy and by specific surface area and cation exchange capacities measurements. Effects of pH, concentration of metal cations and contact time were analysed. The adsorption was strongly dependent on pH of the medium, and the uptake of adsorbed metal increased from pH 2.0 to 6.5, while the solubility of Cu at higher pH values decreased. The uptake of Cu²⁺ was rapid and it increased with increasing metal concentration, while the relative amount of adsorbed Cu²⁺ decreased. The equilibrium adsorption capacity of the adsorbents used for Cu²⁺ was extrapolated using the linear Freundlich and Langmuir adsorption isotherms. The Langmuir isotherm was found to fit better the experimental data measured for both bentonites.

INTRODUCTION

Contamination of the environment from various sources (old mining loads, mining and ore processing, industrial activities, agrochemicals, algaecides preparations) has become an increasingly serious problem in recent years. Majority of heavy metal ions are toxic and harmful even at low concentrations, seriously affecting animals and plants and causing a large number of diseases. Therefore, elimination of these metals from water is important to protect public health and the environment.

Copper is essential to human life and health, but becomes toxic to living organisms at low pH. Thus it is important to remove the excessive amounts of copper present in wastewater in order to prevent pollution of the surface water and groundwater. The most important techniques used for removal of heavy metal ions from wastewaters include chemical precipitation, ion-exchange, adsorption, membrane filtration, coagulation, flocculation, reverse osmosis, flotation and electrochemical methods [1]. Adsorption is one of the mostly utilized processes for the removal of heavy metals from wastewaters. The important properties of the adsorbents include high surface area and loading capacity. Various substances, such as activated carbon, ion exchange resins, zeolites and bentonites have been used as adsorbents for removal of heavy metals from wastewater [2].

The main constituent of bentonite is montmorillonite, a clay mineral from the smectite group, composed of layers made up of two tetrahedral sheets with prevailing Si as the central atom and sandwiching an octahedral sheet with mainly Al in the octahedrons. Because of the isomorphous substitutions in the layers, they bear a negative charge. In montmorillonites, by definition prevails octahedral charge caused by Mg(II) partially replacing the dominating Al(III) in the octahedrons. The negative charge is balanced by hydrated exchangeable cations adsorbed between the layers and on the external surfaces of the particles.

Recently, bentonites have been widely used to remove Cu²⁺ from waste water [3]. Competitive sorption of Cu²⁺, Cd²⁺ [4] and Cu²⁺, Ni²⁺ [5] onto natural bentonites were also thoroughly discussed. For enhancing the sorption properties of bentonites, several modifications were used, such as by acids [6, 7], sulfates, phosphates [8], ethylenediamine [9] and manganese oxide [10] inducing the increase of adsorbed ions in the interlayer space. Poly(oxo zirconium) and tetrabutylammonium derivatives were shown to be not the appropriate pillaring agents for raising the material`s adsorption capacity [11].

Sorption properties of natural Slovak bentonites as well as of their natrified forms suitable for application in high-level radioactive waste repositories were compared [12-16]. Sorption properties decreased in the

order Jelšový Potok > Kopernica > Lieskovec > Lastovce > Dolná Ves. Natrification as a technological process improving bentonite quality can not be used for applications in engineering barriers due to negative impact of basic pH on sorption.

The aim of this work was to investigate the effect of solution pH, time and metal concentration on the adsorption of Cu^{2+} on industrial products from Slovak bentonites.

EXPERIMENTAL

Materials

Two industrial products made from two Slovak bentonites Jelšový Potok (JP) and Lieskovec (L) were provided by the Envigeo, Ltd, Slovakia. Another sample based on Jelšový Potok bentonite (sep.Na-JP) underwent first an industrial treatment on a cyclone classifier to reduce the material to particle size < 250 μm [17]. The < 2 μm fraction was separated by sedimentation from suspension in 1 mol.dm^{-3} NaCl solution. The excess ions were washed out with deionized water and the clay was dried at 60°C. Its major component was a montmorillonite of structural formula $Na_{0.74} Ca_{0.05} K_{0.04} (Al_{3.07} Fe_{0.40} Mg_{0.53}) (Si_{7.62} Al_{0.38}) O_{20}(OH)_4 . nH_2O$. It was characterized in detail in [17] and used here for comparative reasons. All samples were sieved through a 200 μm sieve and dried at 105°C. They were transferred into small polypropylene containers and stored in a desiccator prior to next use.

All used chemicals were of analytical reagent grade. Water deionised by reverse osmosis (Demiwa, Watek Czech Republic) was used for the treatments. Stock solution of Cu^{2+} was prepared by dissolving $CuSO_4.5H_2O$. The pH values of the solutions were adjusted by addition of 0.1 mol.dm^{-3} HNO_3 or NaOH.

Methods

Characterization of adsorbents

Specific surface area was determined by the ethylene glycol monoetyl ether (EGME) method. In this procedure, ~0.25 g of samples was placed in glass weighing cans and dried to constant weight over P_2O_5 in desiccators under evacuation. Few drops of EGME were added to each sample until they got saturated. After 15 minutes the samples were placed in desiccators over $CaCl_2$, evacuated and repeatedly weighed after 90 minutes evacuating intervals. After each weighing the samples were placed back to the desiccators and re-evacuated. Subsequently, the curves depicting EGME retention versus time of evacuation were plotted and the curve points were used to calculate the specific surface areas [18] of 386, 459 and 510 m^2.g^{-1} for L, JP and sep. Na-JP, respectively.

Cation exchange capacity (CEC) was determined by the ammonium acetate method [19]. Weighed portions of the samples (5 g) and 200 cm^3 of 1 mol.dm^{-3} ammonium acetate were mixed in polyethylene tubes. After 24 hours, each sample was washed by ethanol, filtered and dried, then put into a distillation bank with 2g of MgO and 200 cm^3 of deionized water. Subsequently, 100 cm^3 of the distillate was trapped into a flask containing 5 cm^3 of 4% boric acid and 5 drops of bromcresol green and titrated with 0.1 mol.dm^{-3} solution of HCl. The amount of used HCl was utilised to calculate the CEC, obtaining 0.40, 0.79 and 1.05 mmol.g^{-1} for L, JP and sep.Na-JP, respectively.

A Bruker D8 Advance diffractometer using Cu Kα radiation, a step of 0.05° 2Θ and counting time of 1 s per step was used for mineralogical analysis of the samples. Fourier transform infrared (FTIR) spectra were recorded on a Nicolet 6700 spectrometer. For the spectra in the middle IR region (4000 – 400 cm^{-1}) a DTGS detector, a KBr beam splitter and the KBr pressed – disc technique (1 mg of sample and 200 mg of KBr) were used. The discs were heated in a drying oven overnight at 150°C to minimize the amount of adsorbed water. For the spectra in the near IR region (8000 – 4000 cm^{-1}), a PbSe detector, a CaF$_2$ beam splitter and the DRIFT technique was utilized. All manipulations with the spectra were performed using OMNIC 8.0 software package (Nicolet Instruments Corp.).

Adsorption experiments

Batch adsorption experiments were carried out at 20°C in 250 cm^3 Erlenmeyer flasks by mixing 0.5 g of the adsorbent with 100 cm^3 of Cu^{2+} solution with an initial concentration of 50 mg.dm^{-3} and pH = 5.5 was adjusted. The effect of time was investigated with 5g of adsorbent and 1000 cm^3 of Cu^{2+} solution in a time range of 3 – 240 min. For other experiments the interaction time of 240 min. was used. After reaching the desired contact time, the suspensions were centrifuged and the solutions were analysed for Cu^{2+} by atomic absorption spectrometry (AAS). Concentrations of the metal ions before and after the adsorption were measured by atomic adsorption spectrometer AVANTA Σ (GBC Scientific, Australia) with the acetylene-air flame atomization. The measured data were processed by the GBC Avanta software. The pH values of all solutions were measured by a pH meter Model 340 (WTW, Germany). All experiments were performed in duplicates differing by up to ± 5 %.

The sorption data with the initial concentration of 10-200 mg.dm^{-3} have been correlated with two isotherms models. The Freundlich isotherm was applied in a linear form

$$\log q_e = \log K_F + \frac{1}{n}.\log c_e \qquad (1)$$

where c_e and q_e are the equilibrium concentrations of metal ions in the liquid phase and in the solid phase,

respectively; *n* is Freundlich coefficient related to the adsorption intensity and K_F is a surface adsorption equilibrium constant.

Linear Langmuir isotherms were obtained by the following equation

$$\frac{c_e}{q_e} = \frac{1}{Q_m} \cdot c_e + \frac{1}{b.Q_m} \qquad (2)$$

where *b* is a Langmuir coefficient representing the equilibrium constant related to the adsorbate-adsorbent affinity and Q_m is the maximum adsorption capacity corresponding to the monolayer adsorption capacity.

RESULTS AND DISCUSSION

Characterization of the adsorbents

X-ray powder diffraction

Powder XRD patterns of JP and L (Figure 1) reveal that a dioctahedral smectite with a characteristic diffraction near 62 ° 2θ (d_{060} = 1.49 Å) is the dominant mineral in both samples. Prevailing exchangeable cations in the interlayer space are Ca^{2+} in L, a mechanically treated bentonite with a typical exchangeable cation present in the bentonites from Slovak deposits, and Na^+ in JP, an industrially processed material by addition of 4% soda ash (Na_2CO_3), resulting in prevailing exchangeable Na^+ to Ca^{2+}. The obtained d_{001} values of 15.1 Å and 12.5 Å, respectively, are usual for dried Ca^{2+} and Na^+ montmorillonites [20]. Presence of carbonates in JP is confirmed by the diffractions at 28.4° and 29.4° 2θ. The first one near 28.4° 2θ is of higher intensity and broader shape, probably due to contribution of more carbonates diffracting in this area. The diffraction at 29.4° 2θ is assigned to $CaCO_3$ [20] formed by cation exchange reaction between Ca^{2+} cations from montmorillonite and CO_3^{2-} from soda ash. Further admixtures in both samples include quartz, mica and feldspars, while L contains also kaolinite and cristobalite.
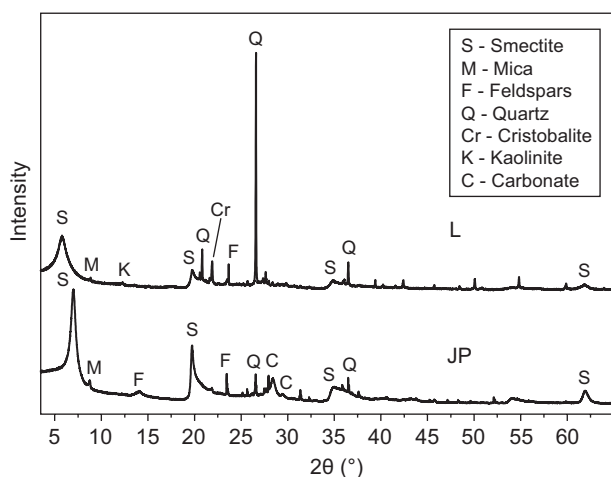
Infrared spectroscopy

MIR spectra (Figure 2) provide further information on the minerals present in the samples as well as on chemical composition of the main mineral. The kaolinite stretching OH vibration at 3698 cm⁻¹ is of higher intensity in the spectrum of L confirming more kaolinite in L than in JP, as has been indicated also in the XRD patterns. Madejová *et al.* proved the ability of IR spectroscopy to detect as few as 0.5 mass % of kaolinite component in the mixtures with montmorillonite [21]. Absorption near 800 cm⁻¹ appearing in the spectra of L and JP samples is assigned to overlapping vibrations of quartz and amorphous SiO_2 [21,22]. The broad band near 1480 cm⁻¹ in the spectrum of JP proves the presence of carbonates, while the bands near 3430 and 1630 cm⁻¹ are attributed to the OH vibrations of molecular water [23]. The strong band near 1035 cm⁻¹ is typical for stretching Si-O vibrations of smectites; however, it may include contributions due to absorption bands of other silicates [22]. The bands at 526 and 469 cm⁻¹ are assigned to AlOSi and SiOSi bending vibrations, respectively. The vibrational band near 3626 cm⁻¹, assigned to stretching AlAlOH vibrations is typical for Al-rich dioctahedral layered minerals, but the presence of Fe^{3+} cations in the octahedra shifts the OH stretching vibrations to lower values [22]. The bending vibrations of OH groups provide more detailed evidence about octahedral cations sharing the hydroxyl groups and showing separate bands for different species of hydroxyls. AlAlOH vibrations at 914 cm⁻¹ and the AlMgOH band at 854 cm⁻¹ confirm higher extent of Mg (II) for Al (III) substitution in JP than in L. The presence of AlFeOH component near 874 cm⁻¹ and the absence of an AlMgOH band reflects higher Fe (III) and lower Mg (II) contents in the octahedra of L, thus contributing to its lower CEC [24]. The relatively high intensity of the AlFeOH band at 874 cm⁻¹ is influenced by the presence of carbonates in JP.

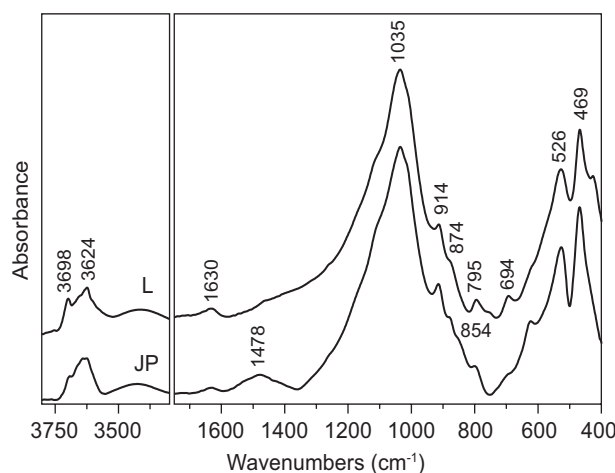Figure 1. X-ray diffraction patterns of JP and L samples.

Figure 2. The MIR spectra of JP and L.

Hence, the Fe content cannot be estimated from this absorption. For more information on the OH groups, IR spectroscopy in the near infrared (NIR) region was used. Figure 3 reflects the first overtones and combination $2\nu_{OH}$ and $(\nu + \delta)_{OH}$ modes of fundamental stretching and bending vibrations in the 8000-4000 cm^{-1} region [25]. The absorption at 7069 cm^{-1} corresponds to the first overtone of AlAlOH vibrations [26]. The first overtone of water molecules with strong hydrogen bonds appears near 6848 cm^{-1}. The strong band near 5240 cm^{-1}, assigned to a combination of the water stretching and bending vibrations is seen in the spectra of both samples. The bands at 4529 cm^{-1} and 4467 cm^{-1} belong to combination modes $(\nu + \delta)_{AlAlOH}$ and $(\nu + \delta)_{AlFeOH}$, respectively [26]. The higher intensity of $(\nu + \delta)_{AlAlOH}$ and absence of $(\nu + \delta)_{AlFeOH}$ in JP indicates that Fe content in this sample is much lower than in L.
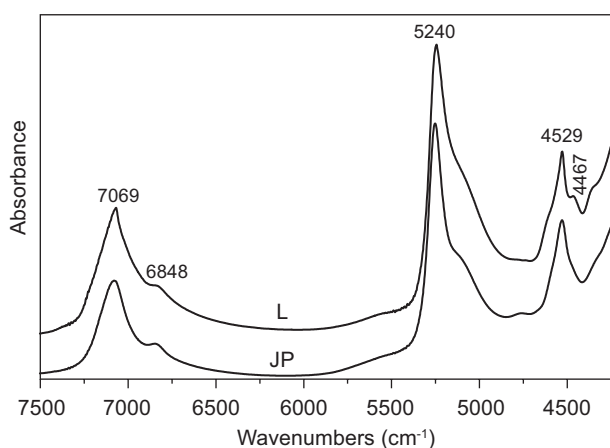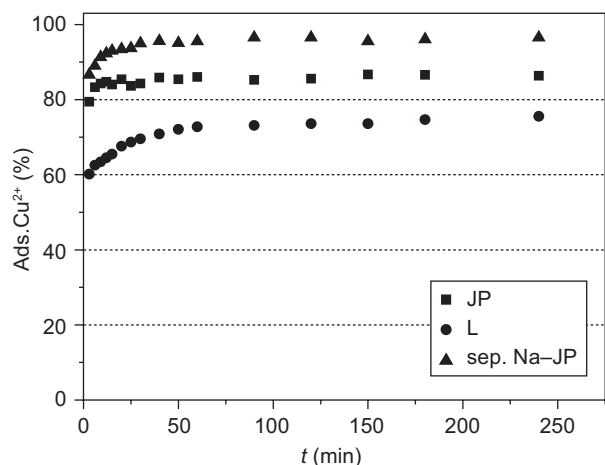

Figure 3. The NIR spectra of JP and L samples.

Figure 4. Time dependence of Cu^{2+} adsorption on JP, L and sep. Na-JP.

Adsorption experiments

Effect of time

The effect of contact time on the adsorption of Cu^{2+} ions on the samples is depicted in Figure 4. A rapid initial uptake of Cu^{2+} ions occurred led to adsorption of over 87, 79 and 60% of total Cu^{2+} ions present in the system by sep.Na-JP, JP and L, respectively, within the first few minutes of the process. In the next 30 minutes followed slower adsorption up to 95, 84 and 70% of total Cu^{2+} ions, respectively. No further changes in adsorbed Cu^{2+} took place in the following 30 min. The whole process of Cu^{2+} removal was described by two distinctive reactions for Cu^{2+} sorption on bentonite. The first reaction covered a rapid exchange of Cu^{2+} with the cations on the surfaces and the interlattice edges, followed by a slower reaction of Cu^{2+} diffusion into the pores [27].

Effect of pH

The pH of solution is a significant parameter in the adsorption processes. In highly alkaline environment heavy metal ions can be transformed to hydroxides that are hardly soluble and they precipitate. The precipitation of Cu^{2+} ions became significant at pH > 6. Hence, the adsorption of Cu^{2+} on bentonite was examined from solution at initial pH values between 2 and 10. The results presented in Figure 5 revealed that the adsorption of Cu^{2+} increased with rising the pH of solution. At pH = 2 preferential H$^+$ sorption was observed for samples JP and L, while it was less evident for sep. Na-JP due to higher CEC of this material. At pH values higher than 6, formation of copper hydroxyl compounds affected the sorption process [28].

Adsorption isotherms

In general, adsorption isotherms provide valuable information on optimizing the use of adsorbing agents. For example, detailed description on affinity between sorbates and sorbents, as well as bond energy and adsorption capacity can be deduced from the isotherm equilibrium models of adsorption processes. Freundlich and Langmuir isotherms are the two most commonly employed models. These were shown to be suitable for description of short-term and monocomponent adsorption of metal ions by different adsorbing materials [30, 31].

Utilization of the isotherm equations was compared on the basis of correlation coefficients R^2. The Langmuir model with R^2 values up to ~ 0.99 yielded in clearly better fits for the adsorption of Cu^{2+} on all studied samples than the Freundlich model (R^2 = 0.78-0.95). The Freundlich adsorption isotherm gives expression encompassing the

surface heterogeneity and the exponential distribution of the active sites, as well as their energies. On the other hand, Langmuir adsorption model is based on the assumption of a sorption on homogeneous surface by monolayer adsorption, while considering no interaction between adsorbed species. Moreover, Langmuir model assumes that the adsorptive forces are similar to the forces of the chemical interaction. Consequently, the Langmuir isotherm is a better applicable model for adsorption of Cu^{2+} on bentonites [17, 32]. Langmuir adsorption constants (Q_m) were calculated from the intercepts and slopes of the linear plots of c_e/q_e vs. c_e (Figure 6). The low value of Q_m for L (7.27 mg.g⁻¹) indicates fewer adsorption sites, what is related to the lower smectite content in this sample and its lower cation exchange capacity. Higher Q_m for JP of 23.75 mg.g⁻¹ shows better accessibility and more adsorption sites in JP. As expected, Q_m of sep. Na-JP (28.33 mg.g⁻¹) was even higher than the value obtained for JP.
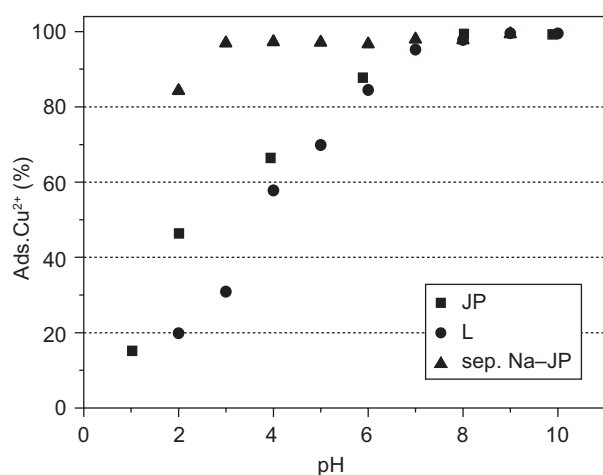
CONCLUSIONS

The adsorption of Cu^{2+} on Slovak industrial bentonite products was investigated and compared with sorption on a separated material. The major mineral component in both industrial products is a montmorillonite. Non-smectitic admixtures in the samples could affect their sorption properties. Uptake of Cu^{2+} by bentonites is rapid and dominated by ion exchange process. The pH is an important factor affecting the adsorption of Cu^{2+}, thus influencing the affinity of the adsorption sites for copper. At pH > 6, the formation of copper hydroxyl compounds affects the sorption. The Langmuir isotherm has been found to fit better than the Freudlich isotherm the experimental data for all samples. The results indicate that industrial bentonite products could be successfully utilized for the adsorption of Cu^{2+} from aqueous solutions and can be effectively used for the removal of copper from wastewater.

Figure 5. Effect of pH on adsorption of Cu^{2+} on JP, L and sep. Na-JP.

References

1. Fu F., Wang Q.: J. Environ. Manage. *92*, 407 (2011).
2. Bhatacharya A.K., Mandal S.N., Das S.K.: Chem. Eng. J. *123*, 43 (2006).
3. Ding S., Sun Y., Yang C., Xu B.: Min. Sci. Technol. *19*, 489 (2009).
4. Karapinar N., Donat R.: Desalination *249*, 123 (2009).
5. Liu Z., Zhou S.: Process. Saf. Environ. *88*, 62 (2010).
6. Vengris T., Binkien R., Sveikauskait A.: Appl. Clay Sci. *18*, 183 (2001).
7. Eren E, Afsin B.: J. Hazard. Mater. *15*, 682 (2008).
8. Olu-Owolabi B.I., Unuabonah E.I.: Appl. Clay Sci. *51*, 170 (2011).
9. Kozák O., Praus P., Machovič V., Klika Z.: Ceramics – Silikáty *54*, 78 (2010).
10. Eren E.: J. Hazard. Mater. *159*, 235 (2008).
11. Bhattacharyya K.G., Gupta S.S.: Sep. Purif. Technol. *50*, 388 (2006).
12. Galamboš M., Kufčáková J., Rajec P.: J. Radioanal. Nucl. Chem. *281*, 485 (2009).
13. Galamboš M., Paučová V., Kufčáková J., Rosskopfová O., Rajec P., Adamcová R.: J. Radioanal. Nucl. Chem. *284*, 55 (2010).
14. Galamboš M., Kufčáková J., Rajec P: J. Radioanal. Nucl. Chem. *281*, 347 (2009).
15. Galamboš M., Kufčáková J., Rosskopfová O., Rajec P: J. Radioanal. Nucl. Chem. *283*, 803 (2010).
16. Galamboš M., Rosskopfová O., Kufčáková J., Rajec P: J. Radioanal. Nucl. Chem. *288*, 765 (2011).

Figure 6. Langmuir isotherm JP, L and sep.Na-JP.

17. Andrejkovičová S., Pentrák M., Jankovič Ľ., Komadel P.: Geol. Carpathica *61*, 163 (2010).
18. Carter D.L., Mortland, M.M., Kemper W.D.: *Methods of Soil Analyses: Part 1. Physical and Mineralogical Methods*, 2nd ed., p.413–423, Madison,Wisconsin 1986.
19. Andrejkovičová S., Madejová J., Czímerová A., Galko I., Dohrmann R., Komadel P.: Geol. Carpathica *57*, 371 (2006).
20. Brown G.: *Crystal structures of clay minerals and their X-ray identification*, Mineralogical Society, London 1980.
21. Madejová J., Kečkéš J., Pálková H., Komadel P.: Clay Miner. *37*, 377 (2002).
22. Farmer V.C.: *Infrared spectra of minerals*, Mineralogical Society, London 1974.
23. Madejová J., Komadel P., Číčel B.: Geol. Carpathica – series clays *1*, 9 (1992).
24. Madejová J., Kraus I., Komadel P, Geol. Carpathica – Series Clays *4*, 23 (1995).
25. Bishop J.L., Murad E., Dyar M.D.: Clay Miner. *37*, 617 (2002).
26. Madejová J., Pentrák M., Pálková H., Komadel P.: Vib. Spectrosc. *49*, 211 (2009).
27. Al-Qunaibit M.H., Mekhemer W.K, Zaghloul A.A., J. Colloid Interface Sci. *283*, 316 (2005).
28. Zhu S., Hou H., Xue Y., Wei N., Sun Q., Chen X.: J. Colloid Interface Sci. *315*, 8 (2007).
29. Abollino O., Aceto M., Malandrino M., Sarzanini C., Mentasti E., Water Res. *37*, 1619 (2003).
30. Oliveira E.A., Montanher S.F., Andrade A.D., Nobrega J.A., Rollemberg M.C.: Process Biochem. *40*, 3485 (2005).
31. Wang X., Zheng Y., Wang A.: J. Hazard. Mater. *168*, 970 (2009).
32. Bhattacharyya K.G., Gupta S.S.: Adv. Colloid Interface Sci. *140*, 114 (2008).